Shape Selective Synthesis of Unusual Nanobipyramids, Cubes, and Nanowires of RuO_2: SnO_2

Niranjan S. Ramgir, Imtiaz S. Mulla, and Kunjukrishna P. Vijayamohanan*

Physical and Materials Chemistry Division, National Chemical Laboratory, Pune 411008, India

Received: July 15, 2004; In Final Form: August 13, 2004

RuO_2 and SnO_2 have a natural habitat of orthogonal/bitetragonal symmetry in the bulk form, which has not been found in the nanodimensions till date. A novel nanobipyramidal structure along with nanowires and cubes of tin oxide has been synthesized by employing RuO_2 as a promoter/nucleating agent. The observation of nanobipyramidal structure in large quantity is striking, emphasizing the stability of these structures. The nanobipyramids are collected in the downstream where the temperature was between 200 and 500 °C, whereas nanowires and cubes are formed on the substrate containing the reaction mixture.

Nanodimensional structures of semiconducting oxides have received considerable attention in recent times because their reduced dimensionality causes a drastic change in the density of states and consequently surface effects become more prominent. For example, several low dimensional structures of SnO_2 like nanorods, nanowires, nanobelts, nanopins, nano-box-beams, and nanodiskettes have been explored recently using various synthetic routes such as thermal evaporation, laser ablation, carbothermal reduction, solution precursor route, etc.[1−13] The method based on the vaporization of oxide materials at high temperature requires a complex apparatus with good vacuum and precise control of temperature and gas flow, and the products are generally collected at the downstream end onto a substrate or inner wall of alumina or quartz tube. Besides size and shape dependent behavior, the doping of nanostructured materials preserving the structural integrity, can provide a far more favorable means of tailoring their properties due to their aspect ratio induced changes in electronic structure.

Because of its unique change in conductance upon adsorption of gases, tin oxide, a wide band gap semiconductor (3.6 eV) is a promising candidate toward miniaturized, ultrasensitive chemical sensors.[8−12] The characteristics of tin oxide containing cations with mixed valences and adjustable oxygen deficiency enables tuning of their structure and properties. For example Meyyappan et al.[13] has shown the synthesis of In-doped tin oxide nanowires using a carbothermal reduction followed by a catalyst mediated heteroepitaxial growth. The doping or compositional changes in nanowires can be controlled by pre-evaporation in a way similar to that in metallorganic chemical vapor deposition (MOCVD). Although several other procedures for synthesizing pristine nanowires have been recently demonstrated, the preparation of doped SnO_2 has not been reported so far, despite its tremendous significance in nanotechnology.

We have successfully synthesized RuO_2 doped SnO_2 nanobipyramids, cubes (which are not reported till date), and nanowires. The importance of the present synthesis lies in its selectivity and simplicity, as it requires neither a sophisticated technique nor a rigorous air-sensitive atmosphere. Moreover, the incorporation of RuO_2 results in the change in the conductance of nanowires illustrating the key role of RuO_2 in controlling the electrical properties of SnO_2.

* Corresponding author. E-mail: viji@ems.ncl.res.in.

SnO_2 in the cassiterite phase belongs to the $P4_2/mnm$ space group and has a ditetragonal bipyramid type of symmetry. The number of macrocrystal habits observed is approximately 10.[14] Figure 1 shows typical micrographs of RuO_2 doped SnO_2 nanobipyramidal structures which also reveal the natural habitat of SnO_2. Upon heating the reaction mixture (RuO_2:SnO) containing 0.1 weight fraction of RuO_2 at 950 °C for 2 h, nanobipyramids are deposited on the alumina substrates that are kept in the temperature range 200−500 °C (Figure 1a−g). No other structure is interestingly found in this region, implying high shape selectivity of the process. Two types of bipyramids are observed, one where the pyramid ends with a tip and the other where a small separation is present between the two opposite triangular planes, suggesting the deviation from the perfect square geometry to be a rectangular one. The bipyramids are polydispersed with size varying between 100 and 800 nm. Most of them are found to be located flat with another end at the backside. The base of the bipyramid is thin with varied dimensions, suggesting the growth process to be initiated from the base, from both sides and growing further, which leads to a pyramid like geometry at the end. Some of them are found lying in different orientations, as shown in Figure 1f, which confirms the bipyramidal nature of the structures. The TEM analysis further confirms that the bipyramids are not monodisperse in nature. Steps at the edge of the structure suggest the growth mechanism to be starting from the edge of cubic structure that is formed prior to the bipyramidal structure. Selected area electron diffraction (SAED) exhibits a kikuchi pattern that can be attributed to the uneven thickness of the structure and the orientation being not parallel to the incident beam. This is due to the electrons that are first scattered inelastically and then elastically from a thick crystalline sample, forming a system of kikuchi lines.

The rutile structure of pure SnO_2 is 6:3 coordinated and the bonding between atoms has a relatively strong ionic character. The tetragonal unit cell contains two Sn and four O atoms. Perpendicular to the surface in the [110] direction, the rutile structure is built up from neutral stacked layers of three alternating planes (O), (2Sn + 2O), and (O) with nominal ionic charges of 2−, 4+, and 2−, respectively, in the surface unit cell. The termination of the SnO_2 (110) called a stoichiometric surface with these three planes is possible. Removal of the

10.1021/jp046859a CCC: $27.50
Published on Web 09/03/2004

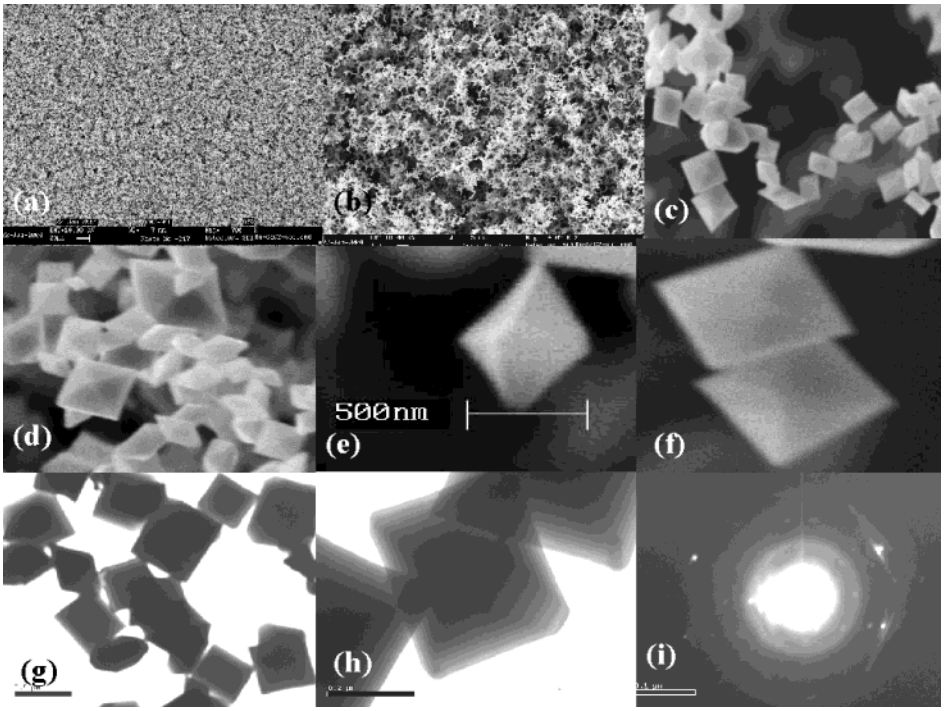

Figure 1. As-synthesized nanobipyramids collected on alumina substrates kept downstream where the temperature is between 200 and 500 °C upon heating the reaction mixture containing 0.1 weight fraction of RuO_2: (a)−(f) SEM images of nanobypyramids; (g) and (h) TEM images; (i) SAED of a single smaller nanobypyramid.

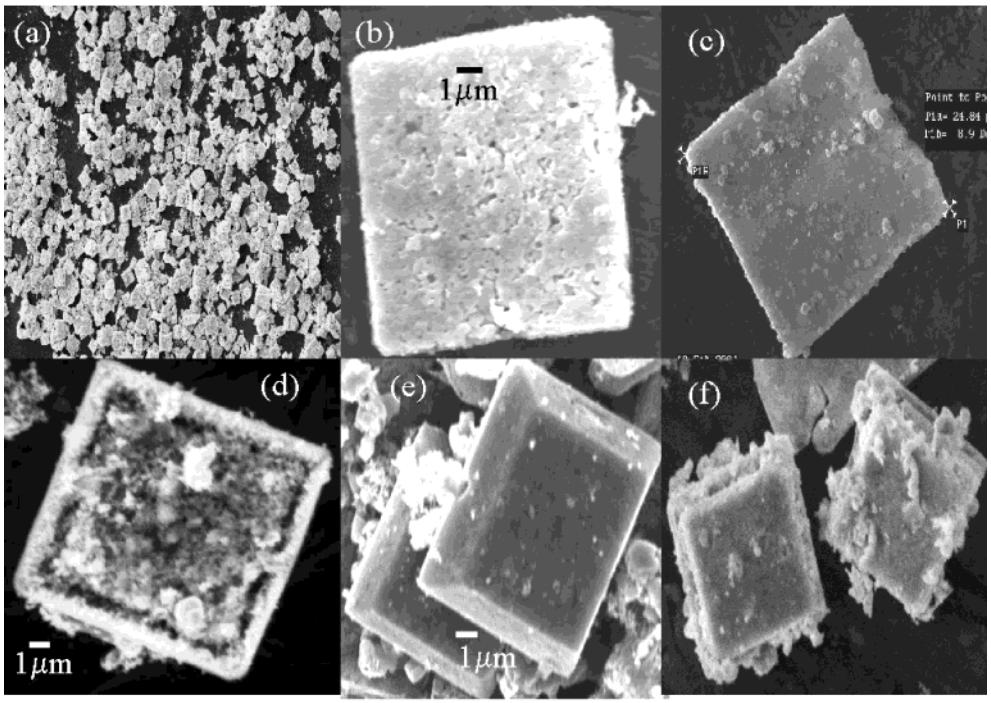

Figure 2. SnO_2 cubes synthesized at 950 °C with 1 wt % of RuO_2 in the reaction mixture: (a)−(d) general SEM images; (e) and (f) biscuit shape.

topmost bridging-oxygen atom results in the reduced (110) surface, which is the case in the nanobipyramidal structure.

For low wt % of RuO_2 in the starting material, nonuniform cubical structures are grown on the substrate containing the reaction mixture (Figure 2). With increase in the RuO_2 percentage in the starting material, the cubes are found to be slowly transformed into nanowires implying Ru to be playing a crucial role as a promoter for 1-D growth of SnO_2. Two types of cubes are observed (RuO_2 1 wt %), one with similar upper and lower surface having dimensions of $a = b = 10-20$ μm and $c = 1-3$ μm. Detailed analysis suggests that the cubes are porous in nature with a diffused boundary. Moreover, the extent of porosity varies from cube to cube that can be attributed to the nonhomogeneity of RuO_2 in the starting material. In some cases well-defined cubic edges with other material just filling in it to give a proper morphology are observed, indicating that the cubic edges are likely to be formed first, followed by their filling to give a complete cubic morphology. The other cubic structure has one surface slightly shorter than the opposite surface, called a biscuit shape, which in the present case accounts nearly 10% of total structures. No such structure formation is observed when experiments are carried out under similar conditions with pure

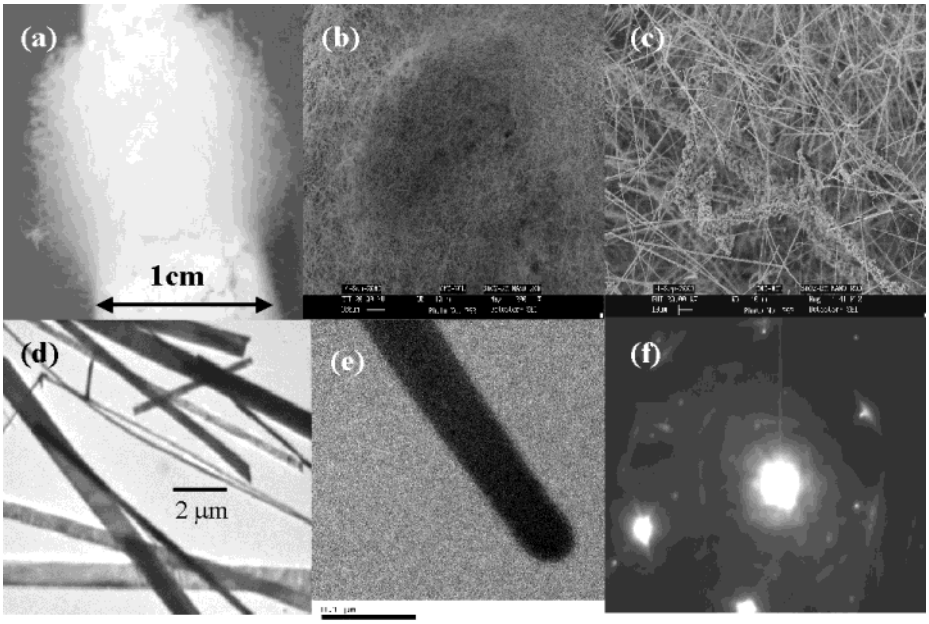

Figure 3. Morphology of as-synthesized nanowires; formed by heating the reaction mixture containing 20 wt % RuO_2: (a) photograph; (b) and (c) SEM images and (d) TEM images of nanowires; (e) rounded tip clearly seen in the TEM image of a single wire; (f) SAED of a single wire of diameter 300 nm.

SnO and RuO_2 individually, which further confirms the role of RuO_2 as a nucleating aid.

Figure 3 shows typical images of the "as-synthesized nanowires" formed by heating the reaction mixture containing 20 wt % RuO_2. Most of the wires appear rather straight, exhibiting smooth sidewalls and detailed examination shows that the wires have width between 100 and 900 nm and length of the order of <1 mm, indicating an aspect ratio of $\sim$1000 (Figure 3b). This large length of the wire is particularly significant in the field of electronics for making the contacts whose conductivity can be tailored by controlling the level of doping. It is also seen that some of the wires are transformed to a highly porous structure consisting of interconnected nanocrystallites ($\sim$5 nm diameter) due to the incomplete 1-D growth, further supporting the role of Ru as a nucleating agent (Figure 3c). As the nanowires were large, they were picked up on a Cu grid directly by sliding over the "as-synthesized" wires on alumina substrates. Figure 3d shows the TEM image of RuO_2 doped SnO_2 nanowires. The wires are not, however, monodispersed in nature with diameter varying between 100 and 900 nm. A liquid droplet composed of RuO_2 and SnO vapors is likely to form first under the reaction conditions directing the growth of SnO_2 into nanowires. We had shown earlier that the incorporation of Ru in SnO_2 thin film results in the low-temperature crystallization, implying the role of Ru as a promoter/nucleating aid besides sensitizer further supporting the results.[15,16] Figure 3f shows the selected area electron diffraction and most of the wires exhibit a kikuchi pattern like that of the nanobipyramid structure implying the higher crystallinity.

The XRD analysis (SI 1, Supporting Information) shows that both the nanowires and nanobipyramids exhibit diffraction peaks that can be indexed to the crystal planes corresponding to the rutile structure of bulk SnO_2 with lattice constant $a = b = 4.74$ Å and $c = 3.20$ Å for nanowires and $a = b = 4.76$ Å and $c = 3.14$ Å for nanobipyramids. No peak corresponding to Ru is seen, suggesting the incorporation of Ru in the lattice owing to the similar size of Ru and Sn (0.69 and 0.71 Å respectively) (SI 2). One peak corresponding to Al (200) can also be identified, which is attributed to the aluminum sample holder used in XRD system. However, the presence of Ru in the structures was confirmed by X-ray photoelectron spectroscopy.

The growth mechanism of 1-D SnO_2 nanostructures prepared by thermal evaporation is very well described by the vapor−liquid−solid model. It is assumed that the tiny liquid metallic tin droplets act as a catalyst as well as the active sites for the SnO_2 vapor adsorption and subsequent deposition. The presence of a spherical particle at the tip of nanostructures confirms the process. In the present work RuO_2 is assumed to play a crucial role for nucleating the nanostructure formation. With a negligible amount of RuO_2 in the reaction mixture, the appearance of a biscuit-shaped cube suggests that the growth is initiated by slow evaporation directed upward. However, with the increase in RuO_2 percentage the cubes appear to be more porous and deformed further supporting the process. Initially, all the SnO grains are assumed to be covered from all side by the RuO_2 and the growth is supposed to take place through a liquid droplet composed of more RuO_2 and less of SnO vapors, which is likely to form first under the reaction conditions directing the growth of SnO into nanowires. The oxygen partial pressure is sufficient for the formation of SnO_2, whereas in case of nanobipyramids the evaporation of RuO_2 leads to the lifting of smaller cubical structures, with the growth process still in progress, leading to the formation of a tip on either side, giving a pyramid like appearance. These structures are carried by the Ar present in the system to the substrates. The randomness in the size and the orientation suggests that each nanobipyramids is isolated, formed separately, and carried away by the carrier gas. The change in the flow rate does not have a noticeable effect on the morphology of cubes, nanowires, or the nanobipyramids. Experiments carried out with different compositions of RuO_2 in the reaction mixture indicate that the nanowire percentage increases with an increase in RuO_2. Moreover, it is possible to control the diameter and length of nanowires by varying the RuO_2 weight percentage and the duration of heating. Nature of carrier gas also has a strong influence on nanowires yield and aspect ratio.

An understanding of the growth mechanism of these structures is important for both the creation of new materials as well as

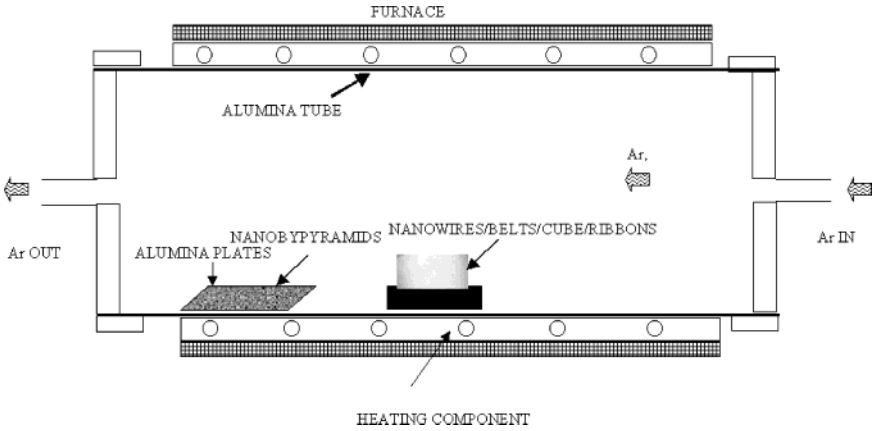

Figure 4.

the fundamental perceptive of devices using these structures. Furthermore, the fabrication process is easy and cost-effective, as the synthesis is carried out in a tubular furnace open at one end, which does not require any controlled atmosphere and instrumentation. We believe that the present work demonstrates for the first time an ability to exert a simple control over the shape and electrical properties of the nanostructures. The systematic variation of RuO_2 percentage in the starting material results in nanowires with different resistance values that vary between 10^9 and $10^3\Omega$. (SI 3) This shows that the electrical properties of tin oxide nanostructures can be tailored using different concentration of doping elements. Some of the wires also exhibit room-temperature sensitivity of 3 orders of magnitude toward NO_2, suggesting their potential use in chemical sensing. As compared with nanowires, which exhibit very high sensitivity ($s = 8075$), cubes show reasonable sensitivity ($s = 1500$) whereas nanobipyramids exhibit still lower average sensitivity ($s = 180$) (SI 4). This can be attributed to the isolated nature of individual nanobipyramids and cubes as revealed clearly in the SEM images. Consequently, these results further suggest the possibility of tailoring the sensitivity by shape control and we believe that this type of study concerning the shape evolution of nanocrystals will be valuable to design and develop advanced nanoscale building-block architectures.

Although the detailed growth mechanism of cubes, nanobipyramids, and nanowires is yet to be confirmed, these structures have significant scientific and technological implications: chemical sensors, building blocks/templates for many functional nanodevices related to fields such as batteries and fuel cells. In summary, we have demonstrated clearly the shape-controlled synthesis of doped tin oxide nanobipyramids, cubes, and nanowires using a simple method of thermal oxidation. These nanowires and nanobipyramids represent good candidates for both further studies of low dimensional physics and the applications in various fields such as nanoelectronics, nanosensors, etc. Our studies further open up the possibility of using present synthesis methodology for the preparation of other doped oxides.

Experimental Section

Figure 4 shows an experimental setup used for the synthesis of nanowires and nanobipyramids. It consists of a tubular furnace open at one end, in which the starting material, a mixture of SnO and RuO_2 in a ratio of 1:0.2 is kept in the middle. Ar is passed continuously at a flow rate of 100 ± 5 sccm through the furnace up to 950 °C. The material was heated for 2 h, and the furnace was allowed to cool naturally with uninterrupted Ar flow. The cubes and nanowires are grown on an alumina boat kept in the middle of the furnace whereas the nanobipyramidal structure is collected on the alumina substrates kept near the end of tube where the temperature is between 200 and 500 °C.

The structure and the morphology were characterized using a scanning electron microscope equipped with energy-dispersive X-ray analysis attachment (A Lieca Stereoscan 440 model SEM with a Kevex model EDAX system), X-ray diffractometer (XRD, Philips 1730 machine), and a transmission electron microscope (Philips CM200 FEG microscope).

Supporting Information Available: XRD of nanobipyramids and nanowires, XPS of nanowires, $I-V$ measurement of nanowires with different levels of RuO_2 doping, distribution of diameter and average length of nanowires, SEM pictures of nanowires in different environments, and shape dependent sensing response toward 500 ppm of NO_2 at room temperature. Contents: **SI 1**, XRD of (a) conventional SnO_2, (b) nanowires, and (c) nanobipyramids; **SI 2**, XPS of (a) Ru, (b) oxygen, and (c) Sn; **SI 3**, $I-V$ measurements of samples with different compositions of RuO_2 in the reaction mixture; **SI 4** (Table 1), distribution of diameter and average length of nanowires calculated for 10 nanowires; **SI 5**, SEM images of nanowires upon heating the reaction mixture containing 0.2 wt % RuO_2 in the presence of (a) Ar, (b) N_2, and (c) O_2; **SI 6**, shape dependent response of RuO_2:SnO_2 toward 500 ppm of NO_2 at room temperature. This material is available free of charge via the Internet at http://pubs.acs.org.

References and Notes

(1) (a) Wang, Z. L.; Kang, Z. C. *Functional and smart materials-structural evolution and structure analysis*; Plenum Press: New York, 1998. (b) Special issue on nanoscale materials. *Acc. Chem. Res.* **1999**, *32*, No. 2.

(2) Xia, Y.; Yang, P.; Sun, Y.; Wu, Y.; Mayers, B.; Gates, B.; Yin, Y.; Kim, F.; Yan, H. *Adv. Mater.* **2003**, *15*, No. 5, 353.

(3) Cui, Y.; Duan, X.; Hu, J.; Lieber, C. M. *J. Phys. Chem. B* **2000**, *104*, 5213.

(4) Scott, R. W. J.; Yang, S. M.; Chabanis, G.; Coombs, N.; Williams, D. E.; Ozin, G. A. *Adv. Mater.* **2001**, *13*, No. 19, 1468.

(5) (a) Wang, Z. L. *Adv. Mater.* **2003**, *15*, 5 432. (b) Dai, Z. R.; Gole, J. L.; Stout, J. D.; Wang, Z. L. *J. Phys. Chem. B* **2002**, *106*, 1274. (c) Dai, Z. R.; Pan, Z. W.; Wang, Z. L. *Solid State Comm.* **2001**, *118*, 351. (d) Dai, Z. R.; Pan, Z. W.; Wang, Z. L. *J. Am. Chem. Soc.* **2002**, *124*, 8637.

(6) Law, M.; Kind, H.; Messer, B.; Kim, F.; Yang, P. Angew. *Chem. Int. Ed.* **2002**, *41*, No. 13, 2405.

(7) Wang, Y.; Jiang, X.; Xia, Y. *J. Am. Chem. Soc.* **2003**, *125* (52), 16176.

(8) Maiti, A.; Rodriguez, J. A.; Law, M.; Kung, P.; Mckinney, J. R.; Yang, P. *Nano Lett.* **2003**, *3* (8), 1025.

(9) Kolkamov, A.; Zhang, Y.; Cheng, G.; Moskovits, M. *Adv. Mater.* **2003**, *15*, No. 12, 997.

(10) (a) Zheng, M.; Li, G.; Zhang, X.; Huang, S.; Lei, Y.; Zhang, L. *Chem. Mater.* **2001**, *13*, 3859. (b) Sun, S. H.; Meng, G.; Zhang, M. G.; An, X. H.; Wu, G. S.; Zhang, L. D. *J. Phys. D: Appl. Phys.* **2004**, *37*, 409.

(11) Hu, J. Q.; Ma, X. L.; Shang, N. G.; Xie, Z. Y.; Wong, N. B.; Lee, C. S.; Lee, S. T. *J. Phys. Chem. B* **2002**, *106*, 3823.

(12) Xu, C.; Zhao, X.; Liu, S.; Wang, G. *Solid State Commun.* **2003**, *125*, 301.

(13) Lui, Y.; Dong, J.; Liu, M. *Adv. Mater.* **2004**, *16*, No. 4, 353.

(14) Hurlburt, C. S.; Klien, C. D. *Manual of Mineralogy*; J. Wiley & Sons: New York, 1985.

(15) Nguyen, P.; Ng, H. T.; Kong, J.; Cassell, A. M.; Quinn, R.; Li, J.; Han, J.; Mcneil, M.; Meyappan, M. *Nano Lett.* **2003**, *3*, No. 7, 925.

(16) (a) Niranjan, R. S.; Sainkar, S. R.; Vijayamohanan, K.; Mulla, I. S. *Sens. Actuators B* **2002**, *82*, 1, 82 (b) Niranjan, R. S.; Mulla, I. S. *Mater. Sci. Eng. B* **2003**, *103*, 103.